

Supporting Information

Separation of lattice-incorporated Cr(VI) from calcium carbonate by converting the microcrystals into nanocrystals via carbonation pathway: based on density functional theory study of incorporation energy

Xiaofeng Mo, Xueming Liu, Jianxin Chen, Shengcai Zhu, Wenbin Xu, Kan Tan, Qingwei Wang, Zhang Lin, Weizhen Liu

1. Pretreatment and characterization

Digestion was conducted for elemental concentration testing based on the standard of Soil and sediment - Digestion of total metal elements - Microwave assisted acid digestion method (HJ 832-2017), samples were mixed with a mixture of HCl-HNO₃-HF and digested at 120°C-190°C. The toxicity leaching experiments were performed by method of Solid waste - Extraction procedure for leaching toxicity - Sulphuric acid & nitric acid method (HJ/T 299-2007), using a sulfuric acid nitric acid solution of pH=3.20±0.05 and mixed with samples at a solid-liquid ratio of 1:10, after shaken on a shaker at 200 r/min for 18±2 h, the leachate was filtered to test the concentration of Cr(VI).

The elemental concentrations were determined by inductively coupled plasma optical emission spectrometer (ICP-OES, AVIO 200, PerkinElmer, USA). The concentration of Cr(VI) in supernatants and leachates was tested based on Water quality - Determination of chromium (VI) - 1,5 Diphenylcarbohydrazide spectrophotometric method (GB 7467-87). The sample is dyed using a 1,5 Diphenylcarbohydrazide chromogenic agent and measured at the wavelength of 450 nm using a UV-vis spectrophotometer (UV2550, Japan). Phase composition of the samples was determined by XRD (D8 Advance, Bruker, Germany), using a semiautomatic Rigaku diffractometer (Geigerflex model) and Cu K α monochromatic radiation over a range of 10°~60° (2 θ) in 0.02 step size with an integration time of 0.2 s. The surface morphologies and structures of the samples were observed by field emission scanning

electron microscope (FESEM, Merlin, Zeiss, Germany) in a secondary electron mode, with an accelerating voltage of 20 kV. The elemental distribution of the samples was analyzed using a scanning transmission electron microscopy (STEM, Tecnai G2 F20).

2. Cr(VI)-containing CaCO₃ samples

The practical Cr(VI)-containing CaCO₃ sludge was derived from a chlorate industry company (LanTai sodium industry, Inner Mongolia, China). It had a moisture of about 40% and pH value over 14. The content of main elements shows that the Cr content of this sample is 1014.5 mg/kg (**Table S1**). The Cr(VI) leaching toxicity of this sample was 53.00 mg/L, which was more than 10 times of the limit of hazardous waste standard (5 mg/L, GB 5085.3-2007, China). XRD analysis shows that the main phase component of the sample was CaCO₃, and a small amount of gypsum and sodium chlorate (**Figure S1-a**). Combined with the results of ICP and XRD analysis, the phase composition of practical (**Table S2**).

A washing treatment (DI water, liquid solid ratio of 10:1, stirring for 15 min) was conducted to the practical Cr(VI)-containing CaCO₃ sludge for 8 times to remove impurity phases. As is shown in **Figure S1-a**, gypsum, vaterite and most of the NaClO₃ was removed by DI water and residual mineral was only CaCO₃. Meanwhile, about 70% Cr(VI) was removed after washing treatment and gradually release with acid leaching (**Figure S1-b**). It means that CaCO₃ is an important host mineral of slow-released Cr(VI)

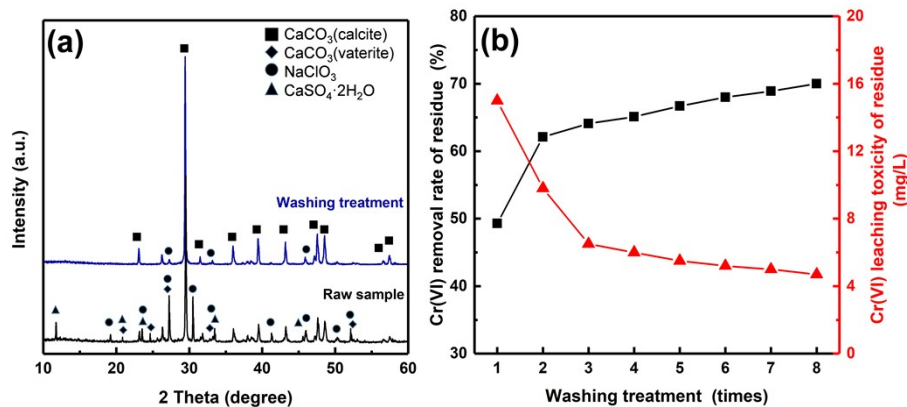


Figure S1. (a) XRD pattern of initial and washed practical CaCO_3 sludge, (b) the Cr(VI) removal rate and leaching concentration of washed residues.

Table S1. The content of main elements in practical Cr(VI)-containing CaCO_3 sludge

| Elements | Cr | Ca | S | K | Mg | Na | Fe |
|----------|--------|--------|-------|-------|--------|--------|-------|
| mg/kg | 1014.5 | 241518 | 14365 | 10284 | 3355.7 | 1290.6 | 190.9 |

Table S2. The phase composition of practical Cr(VI)-containing CaCO_3 sludge

| Components | CaCO_3 | CaSO_4 | $\text{KClO}_3/\text{NaClO}_3$ | $\text{Mg(OH)}_2/\text{MgCO}_3$ | Others |
|------------|-----------------|-----------------|--------------------------------|---------------------------------|--------|
| wt% | 89.0 | 6.1 | 3.3 | 1.17 | 0.5 |

The practical sample was complicated, consisting of many minerals and a variety of metal elements. In order to exclude the influence of irrelevant minerals and metal elements on the mechanism of Cr(VI) separation from CaCO_3 , the Cr(VI)-containing CaCO_3 sample was synthesized via a co-precipitation method according to the production process of the practical Cr(VI)-containing CaCO_3 sludge in the chlorate industry. Specifically, the raw solution (NaCl 117 g/L, Cr(VI) 1000 mg/L) of 1000 mL was prepared, Ca^{2+} (Calcium chloride, 27.75g) and CO_3^{2-} (Sodium carbonate, 26.50g) was added into the solution in sequence. After a sedimentation of 2h, the precipitate was separated, washed by DI water and air dried.

3. Density functional theory (DFT) calculations

The DFT calculations were carried out using the Vienna Ab-initio Simulation

Package (VASP) with the frozen-core all-electron projector-augment-wave (PAW) method. The Perdew-Burke-Ernzerhof (PBE) of generalized gradient approximation (GGA) was adopted to describe the exchange and correlation potential. The cutoff energy for the plane-wave basis set was set to 500 eV. The geometry optimizations were performed until the forces on each ion was reduced below 0.03 eV/Å.

The unit cell of calcite and vaterite were obtained from the Cambridge Crystal Database (CCDC) and the cell parameters are shown in **Table S3**. The unit cells were geometrically optimized by VASP to construct the pure and Cr-doped supercells of calcite and vaterite ($2 \times 2 \times 1$ for calcite and $1 \times 2 \times 1$ for vaterite), Gamma-centered K points were utilized to sample the Brillouin zone of the cells ($3 \times 3 \times 1$ for calcite, $4 \times 2 \times 1$ for vaterite). Besides, the molecular models [CaCO_3 , CaCrO_4 , $\text{Ca}(\text{HCrO}_4)_2$, CaCr_2O_7] used for substitution were also constructed and optimized. The optimized structures used in this calculation were shown in **Figure S2**. Until all the supercell models reached convergence in structural optimization, the Total Energy (eV) of the output structure are obtained. The incorporation energy (E_{inc} , eV) is calculated as follow:

$$E_{\text{inc}} = E(\text{doped}) + E(\text{substituted}) - E(\text{initial}) - E(\text{external})$$

Where, $E(\text{initial})$ and $E(\text{doped})$ are the total energies of the initial and doped structures respectively, and $E(\text{external})$ and $E(\text{substituted})$ are the total energies of the foreign and substituted groups respectively.

Table S3. Unit cell parameters of calcite and vaterite

| Unit cell | $a / \text{Å}$ | $b / \text{Å}$ | $c / \text{Å}$ | $\alpha / (^\circ)$ | $\beta / (^\circ)$ | $\gamma / (^\circ)$ | N |
|-----------|----------------|----------------|----------------|---------------------|--------------------|---------------------|----|
| Calcite | 4.99 | 4.99 | 16.92 | 90 | 90 | 120 | 6 |
| Vaterite | 7.29 | 7.29 | 25.30 | 90 | 90 | 120 | 18 |

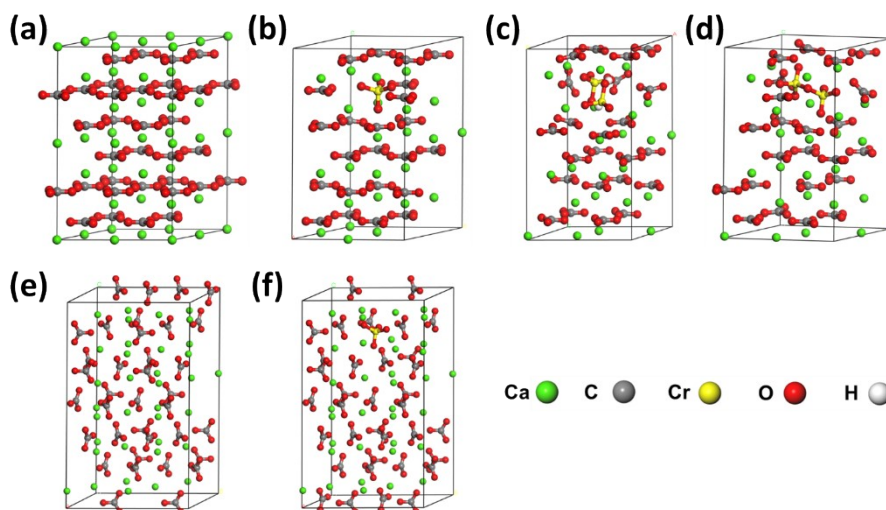


Figure S2. Supercells output after calculation of (a) pure calcite, (b) CrO_4^{2-} -calcite, (c) HCrO_4^- -calcite, (d) $\text{Cr}_2\text{O}_7^{2-}$ -calcite, (e) pure vaterite, (f) CrO_4^{2-} -vaterite

The calculated total energies of 6 supercell models and 4 molecule models for doping established in this DFT calculation are shown in **Table S4**. The calculated incorporation energies of Cr(VI) ionic into CaCO_3 polymorphs are shown in **Table S5**.

Table S4. Total energies of different Cr(VI) species, pure CaCO_3 polymorphs (calcite and vaterite) and different Cr(VI) species-doped calcite and vaterite.

| Groups and Configurations | Total energy (eV) |
|---------------------------------------|-------------------|
| CaCrO_4 | -46.43846181 |
| $\text{Ca}(\text{HCrO}_4)_2$ | -88.26980070 |
| CaCr_2O_7 | -75.66496898 |
| CaCO_3 | -37.36231599 |
| pure-Calcite | -899.59508093 |
| pure-Vaterite | -1347.95872892 |
| CrO_4^{2-} -Calcite | -905.88909377 |
| CrO_4^{2-} -Vaterite | -1354.52422467 |
| HCrO_4^- -Calcite | -946.86410698 |
| $\text{Cr}_2\text{O}_7^{2-}$ -Calcite | -932.07435377 |

Table S5. Cr(VI) incorporation processes and the calculated incorporation energies of

different Cr(VI) species in CaCO₃ polymorphs

| No. | Processes | E _{inc} (eV) |
|-----|---|-----------------------|
| E1 | pure-Calcite + CaCrO ₄ → CrO ₄ ²⁻ -Calcite + CaCO ₃ | 2.78213 |
| E2 | pure-Vaterite + CaCrO ₄ → CrO ₄ ²⁻ -Vaterite + CaCO ₃ | 2.51065 |
| E3 | pure-Calcite + Ca(HCrO ₄) ₂ → HCrO ₄ ⁻ -Calcite + CaCO ₃ | 3.63846 |
| E4 | pure-Calcite + CaCr ₂ O ₇ → Cr ₂ O ₇ ²⁻ -Calcite + CaCO ₃ | 5.82338 |

4. Carbonation experiments

The carbonation experiments were conducted in a small reactor (YZQR-100M, YanZheng Instrument) consisted of a vessel, sealed shell, gas valve, stirrer, pressure gauge and sampling tube. The reaction gas was a liquid CO₂ in a steel cylinder with a volume of 40 L and pressure of 6 MPa. The maximum volume of the vessel was 120 mL, the reaction pressure ranged from 0 to 5 MPa, the stirring rate was set as 200 r/min, and the maximum reaction time was 24 h. The residues were separated using a centrifuge, washed for three times with pure water, and air dried at 105 °C.

The Cr removal rate of treated samples with series of liquid-solid ratios (5:1~50:1) is shown in **Figure S3-a** (The reaction time was set as 24 h, carbonation group was treated with carbon dioxide pressure of 5 MPa, and control group was conducted under air environment). Cr removal rate of series reaction times are shown in **Figure S3-b** (CO₂ pressure of 3 MPa, liquid-solid ratio of 10:1).

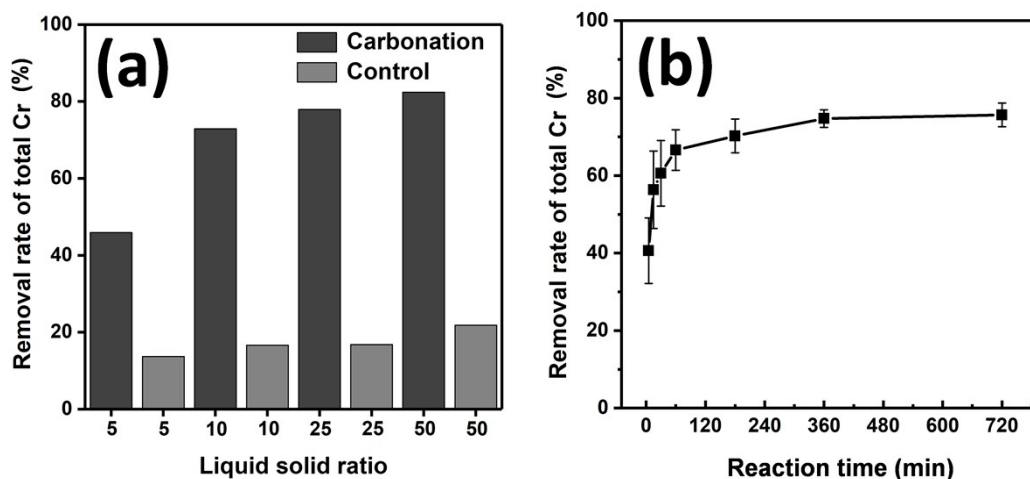


Figure S3. (a) Carbonation and control experiments conducted in series liquid-solid ratio, (b) Cr removal rate of residues during the reaction process

A carbonation reaction conducted in carbon dioxide pressures of 0~5 MPa (0 MPa was carried out in air environment), the liquid-solid ratio was set as 10:1 and the reaction time was 12 h. The concentrations of Ca and Cr were tested via ICP-OES, and the pH value was calculated using software Visual MINTEQ modeling a “CO₂-H₂O-Ca²⁺-Cr(VI)” system. Results are shown in **Figure S4**.

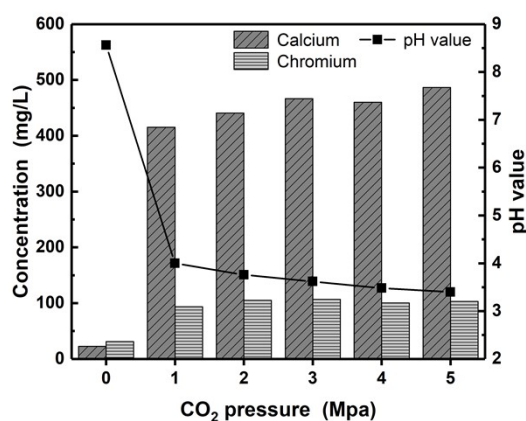


Figure S4. Ca and Cr concentrations of the supernatants in different CO₂ pressure reaction, and the calculated pH value.

5. The Raman spectra characteristic bands of calcite, vaterite and calcium chromate are shown in **Table S6**.

Table S6. Overview of the Raman vibrations observed for the CaCO₃ polymorphs and

| CaCrO ₄ | | | |
|--------------------|---------|---|--|
| mode assignment | Calcite | Vaterite | Calcium Chromate (CaCrO ₄) |
| lattice modes | 156,282 | 124,153, 174,213, 286,277, 310,332 | 111,147, 232,302, 382,464 |
| in-plane bending | 711 | 655,683, 738,744, 751 | / |

| | | | |
|----------------------|------|----------------|---------|
| out-of-plane bending | / | / | 879,905 |
| Symmetric stretching | 1085 | 1074,1081,1094 | / |

Peak positions are given in cm^{-1} .

6. Stability assessment

6.1 Dynamic leaching experiment

Experiment was performed in a glass tube with a clean sand layer at the bottom, the sand layer was covered with filter paper, and the amount of sample added to the glass tube in this experiment was 5.0 g. Based on the leaching standard of HJ/T 299-2007, to simulate the storage environment, a sulfate-nitric acid solution of pH=3.20 was selected as the leaching agent to investigate the leaching behavior. Using a peristaltic pump control to drench the samples at a flow rate of 1 mL/min, and using an automatic sampler to collect an outflow sample every 5 min.

6.2 Stability prediction

The concentration of Cr(VI) of the leachate showed an exponentially decreasing trend, a first-order kinetic model (two-constant model) was used to fit the data and construct a predictive model for the release of Cr(VI) under the specific condition. The equation is

$$C_t = A * V_t^n$$

where C_t (mg/L) is the Cr(VI) concentration of the outflow leachate after leaching time t , V_t (mL) is the total volume of leaching agent at time t , A and n are the fitting parameters.

For $V_t = Q * t$, Q is the flow rate of leaching agent, the amount of released Cr(VI) after a certain leaching time m_t (mg) can be expressed as

$$m_t = \int_{v1}^v C_t dV_t = \int_{t1}^t C_t dt$$

The Cr(VI) release constant L was calculated as

$$L = m_t / m_0$$

where m_0 (mg) is the amount of Cr(VI) in the initial sample.

The functional image of release coefficient equation $L(t)$ (**Figure S5**) were calculated based on the leaching concentration for the initial and treated samples in dynamic leaching experiments.

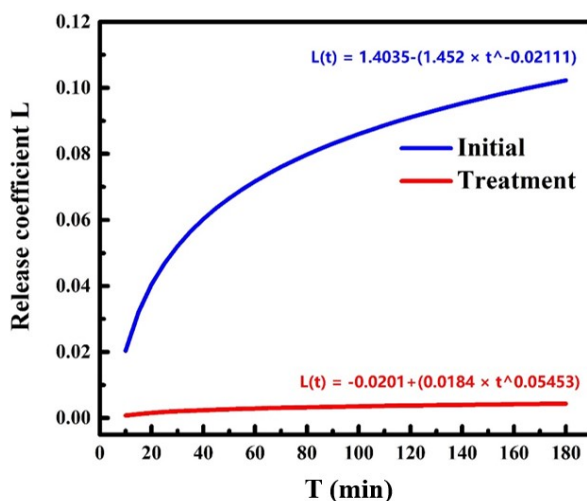


Figure S5. Release coefficient $L(t)$ equations of initial and treated samples

7. Carbonation treatment of actual sample

The carbonation treatment of actual sample is conducted under room temperature with the liquid-solid ratio of 10:1 and reaction time of 24 h. The actual sample was treated under different CO_2 pressures (0~5 MPa, the 0 MPa batch was a control group treated under air condition). As is shown in Figure S6, after treated with 5 MPa CO_2 , the Cr(VI) removal rate of residue was 84.6% and the leaching toxicity decreased to 1.26 mg/L (the disposal limited of which in HJ/T 301-2007 is 1.5 mg/L). In the treated residues, CaSO_4 and NaClO_4 were removed and only CaCO_3 was retained. Same as the synthesized system, the nano CaCO_3 particles were also found in the treated actual sample.

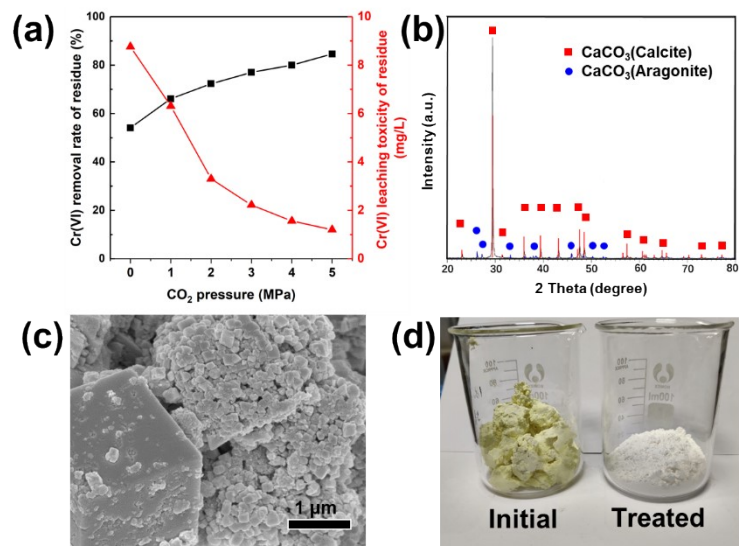


Figure S6. (a) Cr(VI) extraction efficiency and leaching toxicity of residues under various CO₂ pressures; (b) XRD pattern and (c) SEM image of treated residue; (d) comparison of initial and treated samples.